Colloids and Surfaces A: Physicochem. Eng. Aspects 333 (2009) 187–193

Contents lists available at ScienceDirect

Colloids and Surfaces A: Physicochemical and Engineering Aspects

journal homepage: www.elsevier.com/locate/colsurfa

Conformal switchable superhydrophobic/hydrophilic surfaces for microscale flow control

Anindarupa Chunder[a], Kenneth Etcheverry[b], Ghanashyam Londe[c], Hyoung J. Cho[b], Lei Zhai[a,*]

[a] NanoScience Technology Center and Department of Chemistry, University of Central Florida, Orlando, FL 32826, USA
[b] Department of Mechanical, Materials and Aerospace Engineering, University of Central Florida, Orlando, FL 32826, USA
[c] Department of Electrical Engineering, University of Central Florida, Orlando, FL 32826, USA

ARTICLE INFO

Article history:
Received 8 July 2008
Received in revised form
11 September 2008
Accepted 18 September 2008
Available online 30 September 2008

Keywords:
Hydrophobic
Hydrophilic
Switchable
Surfaces
Microfluidic

ABSTRACT

The development of microvalves is essential to realize a fully integrated system for nano/microliter fluid handling in microfluidic devices. Microvalves that utilize passive fluidic manipulation employ a hydrophobic surface in a microchannel network in which the operation is controlled by the interfacial tension of the liquid–air–solid interface. In order to obtain a switchable valve in microfluidic channels, conformal hydrophobic/hydrophilic and superhydrophobic/hydrophilic thermal switchable surfaces were fabricated by the layer-by-layer deposition of poly(allylamine hydrochloride) (PAH) and silica nanoparticles followed by the functionalization of a thermosensitive polymer-poly(*N*-isopropylacrylamide) (PNIPAAm) and perfluorosilane. A fully integrated microfluidic valve using a thermal switchable superhydrophobic/hydrophilic polymer patch has been fabricated. At 70 °C, the valve is superhydrophobic and stops the water flow (closing status) while at room temperature, the patch becomes hydrophilic, and allows the flow (opening status).

Published by Elsevier B.V.

1. Introduction

Microfluidic devices have various applications in basic biomedical, pharmaceutical research, and chemical reaction and analysis [1–5]. In these devices, microvalves are basic building blocks for creating stop-flow condition. These are used for delivering a sample fluid with precise regulations and flow rates at the reduced scale. Compared to active valves, passive valves are easy to fabricate, and less prone to clogging as they do not include any moving component such as a membrane or a piston inside. Most popular passive valves are capillary hydrophobic valves which rely on the interfacial tension of the valve material and the sample liquid to manipulate liquid flow in microfluidic systems. For example, a hydrophobic material can be integrated inside the channel and used as a valve to stop the liquid flow [6]. Lot of work has been done on hydrogel based microfluidic valves where the valve changes volume in response to the external stimuli to stop the flow [7,8]. Although hydrogels can directly convert chemical energy into mechanical work, which eliminates the requirement of external power source, the fabrication of hydrogels in microfluidics with precise control of position and composition is challenging. On the other hand, switchable valves using "smart surfaces"[9] have been investigated for controlling the flow of liquid, and have attracted increasing attentions [10–16]. The properties of these smart surfaces can be changed by external stimuli [17] such as temperature [18], pH [19], photolumination [20] and electric field [21–23]. These switchable surfaces are based on the modification of the surface with responsive polymer molecules [23] or self-assembled monolayers (SAMs) [24–30]. Such a reversible change of the surface morphology and chemical structures leads to the change of wettability of the surface in response to external stimuli. However, controlling the flow in microfluidic channels requires conformal micron scale valves in selected areas, and all these switchable surfaces and hydrogel based systems are limited by the challenges in micro level fabrication and conformability control. Among various techniques to fabricate conformal coatings, the layer-by-layer (LBL) adsorption of materials through different interactions is now a well-established methodology for creating thin film coatings with precisely tuned physical and chemical properties. This technique involves sequential adsorption of materials that can form intermolecular interactions including opposite electrostatic interactions, [31] hydrogen bondings [32,33] and acid–base interactions [34,35]. Such technique has been employed to fabricate superhydrophilic and superhydrophobic coatings [36–39] and provides

* Corresponding author at: 12424 Research Parkway, Suite 400, Orlando, FL 32826, USA. Tel.: +1 407 882 2847; fax: +1 407 882 2819.
E-mail address: lzhai@mail.ucf.edu (L. Zhai).

0927-7757/$ – see front matter. Published by Elsevier B.V.
doi:10.1016/j.colsurfa.2008.09.044

a promising approach to fabricate conformal smart coatings for microfluidic valves.

A hydrophobic valve utilizes the pressure caused by a hydrophobic patch at the solid–liquid–air interface to stop the liquid flow. The total interfacial energy at the interface, U can be presented as follows:

$$U = A_{sl}\gamma_{sl} + A_{sg}\gamma_{sg} + A_{lg}\gamma_{lg} \quad (1)$$

where A_{sl}, A_{sg} and A_{lg} are solid–liquid, solid–gas, and liquid–gas interface areas, respectively, and γ_{sl}, γ_{sg} and γ_{lg} are their corresponding surface energies per unit area. As the liquid of volume V_L moves onto the hydrophobic patch, A_{sl} increases while A_{sg} decreases. The total energy U is a function of the volume V_L. Therefore, the pressure at the interface can be expressed as

$$P = \frac{-dU}{[dV_L]} \quad (2)$$

The relation between the surface energies and the liquid contact angle θ at the solid–liquid–air interface line is expressed in Young's equation as [40,41]

$$\gamma_{sl} = \gamma_{sg} - \gamma_{lg}\cos\theta \quad (3)$$

The combination of Eqs. (1) and (3) gives

$$U = (A_{sl} + A_{sg})\gamma_{sg} - A_{sl}\gamma_{lg}\cos\theta + A_{lg}\gamma_{lg} = U_0 - A_{sl}\gamma_{lg}\cos\theta + A_{lg}\gamma_{lg} \quad (4)$$

where U_0 is constant because $A_{sl} + A_{sg}$ is constant throughout the process.

Including Eq. (4) into Eq. (2) leads to

$$P = -\frac{\partial U}{\partial V_L} = \gamma_{lg}\left(\cos\theta\frac{\partial A_{sl}}{\partial V_L} - \frac{\partial A_{lg}}{\partial V_L}\right) \quad (5)$$

The liquid will flow over the patch when P is positive, and will stop at the patch when P is negative. If the thickness of the hydrophobic patch is negligible compared with the channel size, $\partial A_{lg}/\partial V_L$ is zero and $\partial A_{sl}/\partial V_L$ is positive. Therefore, P is negative when the patch is hydrophobic since the contact angle is larger than 90°.

On the other hand, the contact angle at the solid–liquid–air interface or the wettability of a solid surface largely depends on both its surface energy and roughness. The liquid wetting behavior on rough surfaces is presented by two classical theories. Wenzel's model [42,43] describes the scenario where the liquid makes a good contact with the rough surface where the roughness increases the contact angle. The contact angle measured on the rough surface (Wenzel's angle θ_w) can be expressed with the contact angle of the liquid on a flat surface obtained from Young's equation and the surface roughness r:

$$\cos\theta_w = r\cos\theta_y \quad (6)$$

In contrast, Cassie-Baxter model describes the wetting behavior of a liquid on a composite surface where a small volume of trapped air below the liquid droplet [44].

$$\cos\theta_c = f_1\cos\theta_1 + f_2\cos\theta_2 \quad (7)$$

where θ_1 is the contact angle for component 1 with fraction f_1 and θ_2 is the contact angle for component 2 with fraction f_2. This equation takes on special meaning when in a two component system with one component being air with a contact angle of 180°. With $f_2 = 1 - f_1$ and $\cos(180^\circ) = -1$, Eq. (7) can be reduced to

$$\cos\theta_c = f_1(\cos\theta_1 + 1) - 1 \quad (8)$$

Since the liquid contact angle on a rough hydrophobic surface is larger than that on a flat hydrophobic surface, a rough hydrophobic surface can generate higher pressure to stop the liquid flow than a flat hydrophobic patch. Such concept is important in designing smart valves that can change their wettability to liquid with external stimuli. For example, poly(*N*-isopropylacryamide) (PNIPAAm) has been widely used in thermal switchable surfaces because PNIPAAm is a thermoresponsive polymer which exhibits its lower critical solution temperature (LCST) in an aqueous solution, and shows a sharp phase transition at ~32 °C.[45–48] PNIPAAm is soluble in water below its LCST (~32 °C), while at temperatures above its LCST, it forms intramolecular hydrogen bonds and becomes insoluble. The water contact angle on a flat PNIPAAm surface is 63° and 92° at 25 and 40 °C, respectively. [23] Such a small contact angle change is not sufficient to manipulate the flow. However, it is clear from Wenzel model that the surface roughness can make a hydrophobic surface more hydrophobic and a hydrophilic surface more hydrophilic. With this concept in mind, we reasoned that a conformal rough patch functionalized with PNIPAAm might be able to function as a thermo-stimulated switchable valve in microfluidic channels.

In this paper, we report the fabrication of a novel thermo-stimulated switchable superhydrophobic/hydrophilic surface and its applications as hydrophobic valves in microfluidic channels. In our studies, the layer-by-layer technique was used to build uniform and conformal multilayer films of poly(allylamine hydrochloride) (PAH) and silica nanoparticles with a precise control of film thickness and roughness. The surface was further functionalized with PNIPAAm and a low surface energy material-(1H, 1H, 2H, 2H-perfluorooctyl)silane (perfluorosilane). The combination of surface roughness and chemical composition created a switchable superhydrophobic/hydrophilic surface. This unique switchable surface was incorporated in a microfluidic channel as a microvalve, and has demonstrated the capability of controlling the flow with the temperature change.

2. Experimental

2.1. Materials and chemicals

Poly(allylamine hydrochloride) (PAH) (M_w ~ 70,000), poly(sodium 4-styrene sulfonate) (SPS) (M_w ~ 70,000) (1H, 1H, 2H, 2H-perfluorooctyl)silane, the colloidal silica nanoparticles Ludox TM-40 (40 wt% SiO_2 suspension in water, average particle size of 22 nm) and Ludox SM-30 (30 wt% SiO_2 suspension in water, average particle size of 7 nm) were obtained from Sigma–Aldrich (St. Louis, MO). Poly(acrylic acid) (PAA) (25% aqueous solution, M_w ~ 90,000) was obtained from Polysciences (Warrington, PA). Deionized water (>18 MΩ cm, Millipore Milli-Q) was used in all aqueous solutions and rinsing procedure.

2.1.1. Fabrication of rough PAH/silica nanoparticle coatings

A rough multilayer film was prepared by the layer-by-layer (LBL) assembly of negatively charged SiO_2 nanoparticle and positively charged PAH on glass substrates at room temperature. In a typical LBL deposition, the substrate was first dipped into a cationic solution for 15 min followed by one 2 min and two 1 min rinsing steps using Milli-Q water. Then, the substrate was dipped into an anionic solution for 15 min, followed by the same rinsing steps. Prior to the deposition of the PAH/SiO_2 layer, the glass substrates were coated with five bilayers of poly(allylamine hydrochloride) and poly(styrene sulfonate), which acted as an adhesive layer between the glass substrate and the PAH/SiO_2 multilayer. The silica solution consisted of 0.069% (w/v) Ludox SM 30 nanoparticle suspension and 0.081% (by w/v) Ludox TM 40 nanoparticle suspension in a 0.1 M NaCl solution. The pH of PAH solution and silica nanoparticle solu-

tion was maintained at 7.5 and 9.0, respectively. The LBL created a rough, multilayered, porous polymer film on the glass substrate. On the top of the rough surface, 3 bilayers of PAH and silica nanoparticles were deposited as a topping layer. The pH of PAH solution is maintained at 7.5. The silica solution consists 0.03% (w/v) Ludox SM 30 nanoparticle suspension. The silica nanoparticles decorated the rough polymer surface and increased its roughness. After the film was annealed, 2 bilayers of PAH (pH 8.5) and PAA (pH 3.5) was deposited onto the film with PAA on the top to provide carboxylate groups to couple the initiator.

2.1.2. Initiator coupling

The initiator solution consisted of 1 g of 2,2′-azobis (2-methylpropionamidine) dichloride (ABMP) and 0.494 g of *N*-(3-dimethlyaminopropyl)-*N*-ethylcarbodimide (EDC) dissolved in 100 ml of water. The glass substrate with the PAA functionalized nanoparticle film was placed into the aqueous solution of the free-radical initiator and allowed to react for 2 h. Such treatment created an initiator layer on the rough polymer film from which the thermosensitive PNIPAAm could be grafted. The initiator-derivatized sample was rinsed in deionized water, dried, and used immediately for polymerization.

2.1.3. Poly(N-isopropylacrylamide) (PNIPAAm) grafting

Thermosensitive PNIPAAm was grafted from the ABMP modified rough surfaces. ABMP modified sample was placed in a 1% NIPAAm aqueous solution, follow by 15 min nitrogen gas purge to remove the dissolved oxygen. 0.135 g of ABAH was then added quickly to the solution and the reaction vessel was sealed immediately. Polymerization reaction was carried out typically at 65 °C which was indicated by the change of the clean reaction solution into a milky white suspension. The sample was removed from the reaction vessel as soon as the solution turned milky to ensure a very thin layer of polymer on the film. Another sample was prepared with 2 h polymerization to deposit a thick layer of PNIPAAm onto the film. The samples were rinsed with deionized water and dried.

The chemical vapor deposition of (1H, 1H, 2H, 2H-perfluorooctyl) silane (perfluorosilane) was performed by put perfluorosilane and the sample under 1 bar vacuum for 45 min.

2.2. Characterization

Atomic force microscopy (AFM) height and phase images were collected using an AFM microscope (Pico SPM) in tapping mode. AFM images were obtained with scan sizes ranging from 500 nm to 1 μm. All images were obtained using tapping mode imaging with a single silicon probe (force constant of 0.5–9.5 N/m). The scan angle was maintained at 0°, and the images were captured in the trace direction with a scan rate of 56–58 kHz. Contact angles were measured using a Goniometer. The morphology of polymer deposited nanoporous film on glass substrate was characterized using JEOL 6400F scanning electron microscopy (SEM) system with an accelerating voltage of 5 kV for imaging. The chemical state of the elements in the SiO_2 nanoparticle incorporated multilayer film and the grafted polymer was studied by X-ray photoelectron spectroscopy (XPS) with a takeoff angle of 90°. The specimen was kept under a vacuum of about 10^{-9} Torr inside the chamber of XPS system. The spectrometer was calibrated using a metallic gold standard ($Au4_{7/2}$ = 84.0 ± 0.1 eV). Charging shifts produced by the samples were corrected by using the binding energy referenced to that of C (1 s) of the adventitious carbon at 284.6 eV.

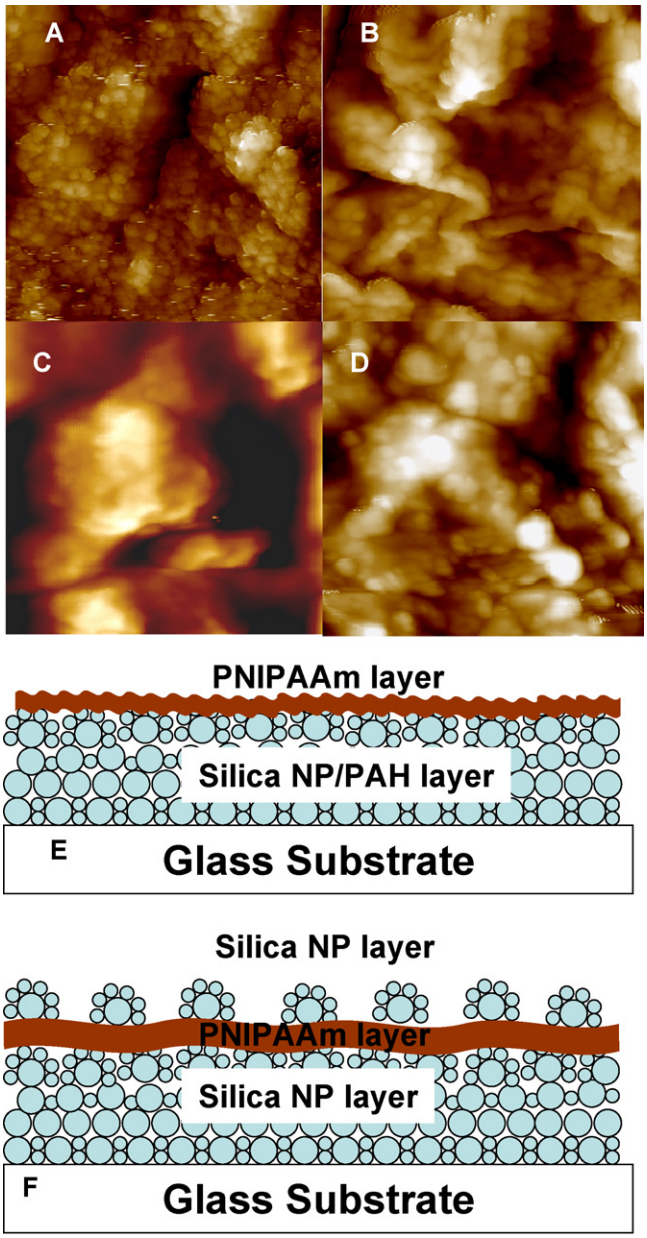

Fig. 1. AFM height images of (A) annealed PAH/SiO_2 multilayer film with dual-length scale structures. (B) A very thin layer of PNIPAAM deposited on rough multilayer film (Sample 2). (C) A thick layer of PNIPAAm deposition after 2 h polymerization which reduces roughness (Sample 2). (D) Nanoscale roughness is reintroduced with silica nanoparticle deposition on the thick PNIPAAm polymer film (Sample 3). (The size of all images is 1 μm.) (E) Schematic illustration of the structure of Sample 2. (F) Schematic illustration of the structure of Sample 3.

3. Results and discussions

A thermally stimulated switchable superhydrophobic/hydrophilic surface requires two components: a dual length scale structure that is necessary for building a superhydrophobic surface and a stable cover layer of thermal switchable molecules such as PNIPAAm. The temperature induced molecular formation change enables the hydrophobic or hydrophilic part of the molecular chain to become exposed to a liquid droplet, leading to different wetting behavior (i.e. hydrophilic and hydrophobic).

In our studies, rough coatings with both micro- and nanostructures were fabricated by depositing 40 bilayers of PAH/SiO_2

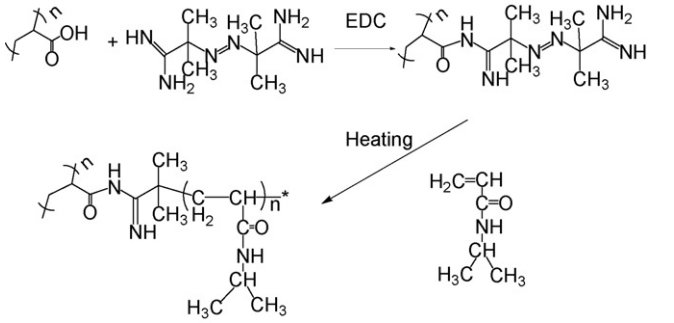

Scheme 1. The synthesis route of grafting PNIPAAm from a surface of PAA.

nanoparticles (a mixture of 22 and 7 nm silica nanoparticles) and 3 bilayers of PAH/SiO_2 (7 nm silica nanoparticles) on glass substrates through the layer-by-layer self-assembling technique [49]. The rough coating was heated at 400 °C for 2 h to anneal the silica nanoparticles to obtain a robust film. From the atomic force microscopy (AFM) image (Fig. 1A) of the film, both micro- and nanostructures can be clearly observed. Additionally, a layer of perfluorosilane was deposited onto the film via a chemical vapor deposition. After the perfluorosilane treated sample was heated at 140 °C for 2 h, it demonstrated superhydrophobicity (advancing contact angle = 163° and receding contact angle = 160°), suggesting that such film can provide the structures to generate superhydrophobicity.

In order to generate a uniform stable PNIPAAm layer on the top of the film, PNIPAAm should be grafted from the rough surface. The radical polymerization of *N*-isopropylacrylamide initiated by 2,2′-azobis (2-methylpropionamidine) dichloride (ABMP) was reported to graft PNIPAAm from surfaces with carboxylate groups. [50] In our studies, since no carboxylate groups were available on the anneal surface to immobilize ABMP, two bilayers of PAH/PAA were deposited onto the annealed film via the LBL technique to introduce carboxylate groups on the surface. ABMP was then coupled with the carboxylate group via a coupling reaction catalyzed by *N*-(3-dimethlyaminopropyl)-*N*-ethylcarbodimide (EDC). The subsequent polymerization of *N*-isopropylacrylamide generated a stable PNIPAAm coating on the top the rough surface (Scheme 1) [50].

As described in the Wenzel model, the surface roughness can increase the hydrophobicity of a hydrophobic surface. Therefore, it is important to control the polymerization time because excess PNIPAAm was expected to fill the pores on the rough surface and reduce the roughness. Two samples with different polymerization time were prepared and examined to reveal the relationship between the surface wetting behavior and surface morphology.

In the polymerization reaction, one sample (Sample 1) was taken out from the reaction solution when the solution turned milky while the other sample (Sample 2) was kept in the reaction solution for 2 h after the solution turned milky. The surface morphology and surface chemical composition of these two samples were examined by AFM and XPS, respectively. Compared with the AFM image of annealed sample (Fig. 1A), the shape of individual silica nanoparticles is still visible in the AFM image of Sample 1 but it is not observable in the AFM image of Sample 2. This suggests that the short polymerization time will lead to a thin PNIPAAm layer on the rough surface while the long polymerization will generate a thick PNIPAAm layer that will fill the pores on the rough surface and eliminate the nanoscale roughness. However, the nanoscale roughness can be easily regenerated by depositing a layer of silica nanoparticles onto Sample 2 by immersing Sample 2 into a silica nanoparticle solution. As shown in Fig. 1D, the silica nanoparticles are visible in the AFM image of the resultant sample (Sample 3).

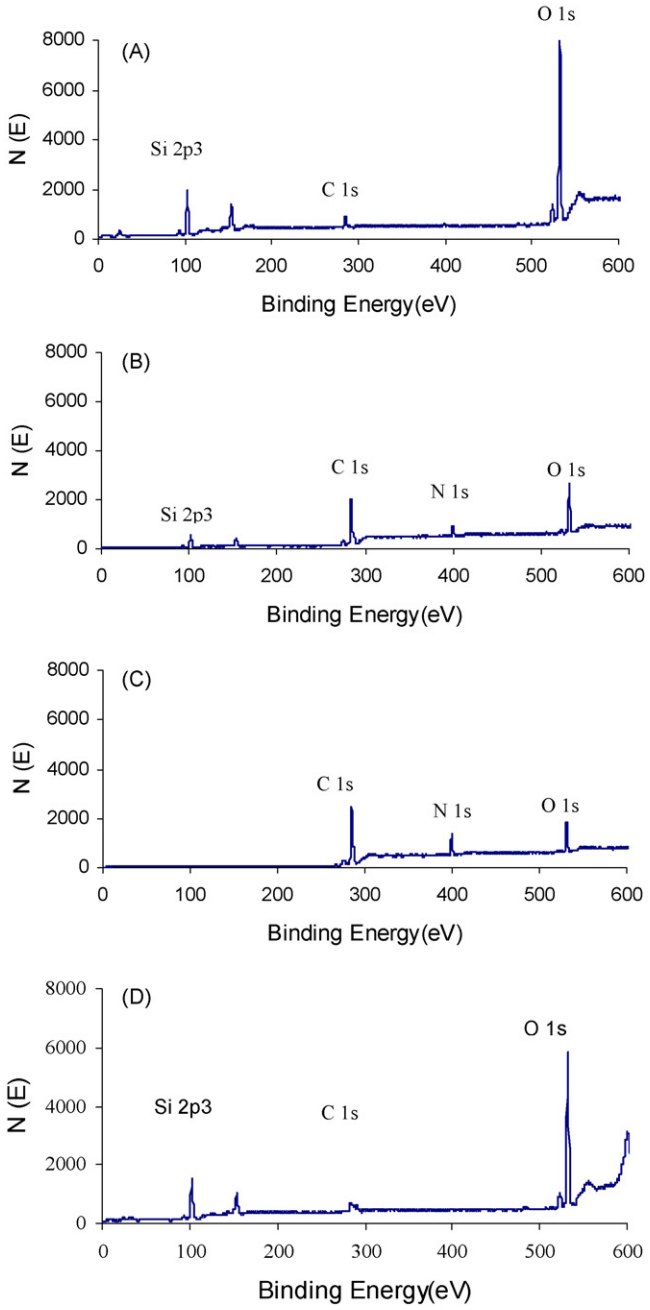

Fig. 2. X-ray photoelectron spectroscopy (XPS) analysis of the surface composition of an annealed silica nanoparticle film (A), a rough silica film covered with a thin layer of PNIPAAm (Sample 1) (B), a rough silica film covered with a thick layer of PNIPAAm (Sample 2) (C) and a rough PNIPAAm functionalized silica film covered with a layer silica nanoparticles (Sample 3) (D).

The XPS survey spectrum of Sample 1 (Fig. 2B) shows the reduction of the Si $2P_3$ peak that is assigned to silica nanoparticles on the annealed film (Fig. 2A) and the appearance of the N peak that is attributed to PNIPAAm, suggesting the formation of a thin layer of PNIPAAm. However, the presence of the Si $2P_3$ peak indicates that the PNIPAAm layer does not cover the surface completely. In contrast, no Si $2P_3$ peak is observed in the XPS survey spectrum of Sample 2 (Fig. 2C), suggesting that the silica layer is completely covered by the PNIPAAm polymer layer. The appearance of Si $2P_3$ peak and the absence of N peak in Fig. 2D indicates that PNIPAAm was covered by silica nanoparticles in Sample 3.

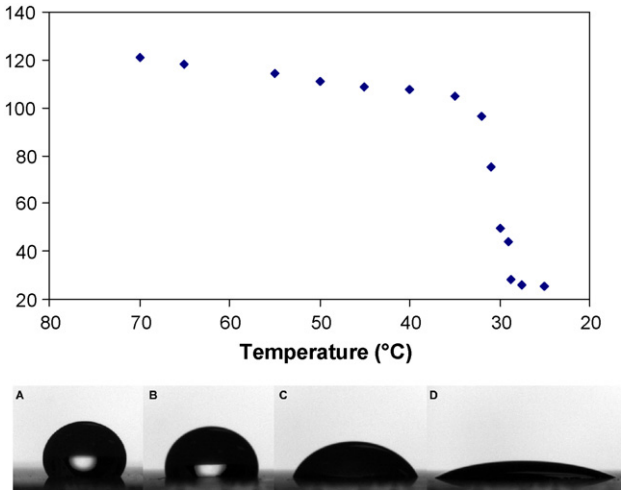

Fig. 3. The change of water contact angle (°) vs. temperature (°C) on a hydrophobic/hydrophilic switchable surface (Sample 1).

The thermo-stimulated switchable wetting behavior of Sample 1 and Sample 2 was investigated by monitoring the change of water contact angle with temperature. Fig. 3 shows the change of water contact angle with temperature for Sample 1. The largest water contact angle is 122° at 70 °C and it decreases with the decrease of temperature. A fast decrease of the contact angle happens around 32 °C (LCST of PNIPAAm) due to the change of the PNIPAAm molecular structure from intramolecular hydrogen bond (hydrophobic) to intermolecular hydrogen bond (hydrophilic). Although a superhydrophobic surface was not obtained from Sample 1, the difference between the largest contact angle (122° at 70 °C) and the smallest contact angle (17° at 20 °C) is 105° which is much larger than that on a flat PNIPAAm surface (29°). This result is consistent with the Wenzel model and suggests that a rough surface can greatly increase the hydrophobic/hydrophilic contrast of a switchable surface. In contrast, the water contact angle changed from 92° to 65° on Sample 2 due to the reduced surface roughness. Sample 3 was superhydrophilic due to the coverage of silica nanoparticles on the surface. After it was coated with perflurosilane, it turned into superhydrophobic but did not show any superhydrophobic/hydrophilic switching properties. We believed that PNIPAAm was buried underneath the silica nanoparticles, and did not contribute to surface wetting properties. Therefore, in order to generate a superhydrophobic/hydrophilic switching surface, silica nanoparticles should not fully cover the PNIPAAm surface, which would allow the exposure of PNIPAAm.

To make a superhydrophobic/hydrophilic switchable surface, a surface roughness and a partial exposure of PNIPAAM was required. The PNIPAAM grafted surface (sample 2) was immersed into a 0.01 M solution of poly(acrylic acid) [PAA] for 1 min followed by dipping into 0.01 M solution of poly(allylamine hydrochloride) [PAH] for 1 min to prepare a adhesive layer for silica nanoparticles on the surface. A layer of silica nanoparticles was then deposited on the Sample 2 surface using a 0.02% silica nanoparticle solution and the short dipping time (2 min) to introduce nanoscale roughness and partially cover the PNIPAAm layer. A layer of perfluorosilane was then deposited on the sample surface followed by the heat treatment to alter the surface wetting properties. The partial coverage of the PNIPAAM was determined and optimized with the help of AFM and testing the switching performance of the surface. High resolution XPS analysis reveals the presence of N on the surface and confirms a scattered deposition of silica nanoparticle onto the PNIPAAm layer (Fig. 4). The thermo-stimulated switchable

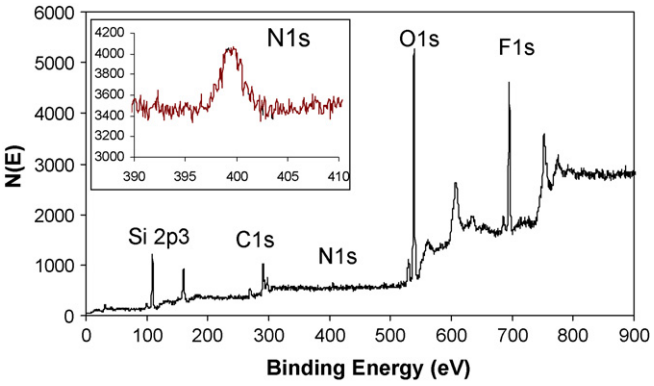

Fig. 4. XPS spectra of Sample 2 partially covered with silica nanoparticle follow by CVD of perfluorosilane. The inset high resolution XPS spectrum shows the presence of nitrogen peak suggesting that PNIPAAm is exposed.

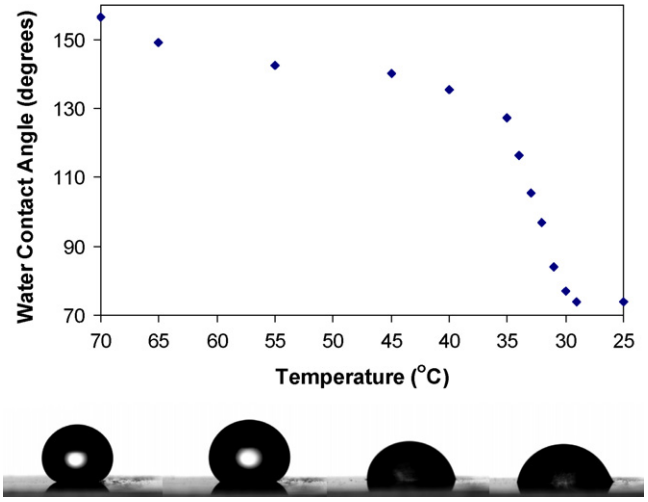

Fig. 5. The change of water contact angle (°) vs. temperature (°C) on a superhydrophobic/hydrophilic switchable surface.

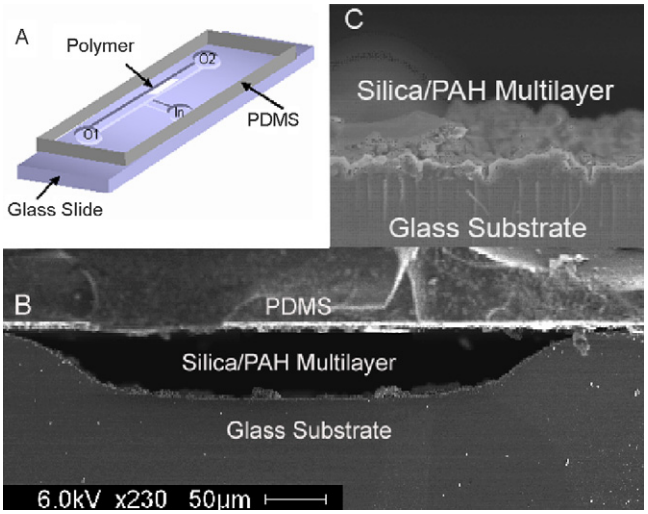

Fig. 6. The schematic illustration of a microfluidic channel with a thermal valve (A); SEM image of the cross section of the etched glass channel with a (polydimethyl siloxane) (PDMS) seal (B) and High resolution SEM image of switchable coatings (C).

wetting behavior of the sample was investigated by monitoring the change of water contact angle with temperature. As shown in Fig. 5, the largest water contact angle is 156° at 70 °C with a receding contact angle of 151°. Such superhydrophobic surface is attributed to the combination of surface structures and hydrophobic silica nanoparticles and PNIPAAm at this temperature. The small hysteresis (5°) suggests that PNIPAAm chains maintain their hydrophobic structures at high temperature with the exposure to water. The water contact angle decreases with the decrease of temperature and reaches 73° at 28 °C. At this temperature, PNIPAAm becomes hydrophilic and change the surface wetting properties. The dramatic contact angle decreasing also happens around 32 °C, which suggests that PNIPAAm turns into hydrophilic at its LCST and changes the surface from hydrophobic to hydrophilic.

The superhydrophobic/hydrophilic switchable surface was used to build a thermo-stimulated valve in a microfluidic channel. The valve was made by wet etching a glass substrate to create channels of around 50 μm in depth (Fig. 6A). A positive photoresist (Microposit S1813, Shipley) was spin coated on the etched glass slide and patterned photolithographically to produce openings for the selective polyelectrolytes deposition on the exposed area of the channel [51]. The superhydrophobic/hydrophilic surface was built by the deposition of different materials according to the following sequence: 40 bilayers of PAH/silica nanoparticles, annealing the sample, 3 bilayers of PAH/PAA, the coupling of initiator 2,2′-azobis (2-methylpropionamidine) dichloride (ABMP) with PAA catalyzed by *N*-(3-dimethlyaminopropyl)-*N*-ethylcarbodimide (EDC), polymerization of NIPAAm, one layer of silica nanoparticles, chemical deposition of perfluorosilane, and heat treatment at 90 °C for overnight. The photoresist was removed using acetone. The channel was sealed with a polydimethyl siloxane (PDMS) slab with three openings (Fig. 6A). The scanning electron microscope images of the channel cross section (Fig. 6B and C) show that the multilayer deposition and subsequent functionalization creates a conformal uniform coating (about 2-μm thick) on the opening of the etched channel. The patch thus created has a dimension of 2 mm × 1.4 mm. For the valve test, the device was heated with the help of a microheater up to a temperature of 70 °C. A programmable syringe pump (Harvard PHD 2000) was used to pump dye-colored water heated at 70 °C at a flow rate of 20 μl/h into the inlet reservoir. As soon as the water entered the channel in the device, the pumping was stopped and the liquid was allowed to flow in the microchannels under capillary action only. Fig. 7B shows the operation of the switchable valve at 70 °C at which the PNIPAAm forms intramolecular hydrogen bonds and becomes superhydrophobic. The dyed water cannot pass over the film surface after it fills a branch of the channel by a capillary effect. This creates the “stop” condition of the valve. Then the heating source was withdrawn and the device along with the water inside was allowed to cool down to room temperature by placing the whole system on a metal plate. The metal plate acted as a heat sink and the temperature decreased to 30 °C in 15 min. PNIPAAm forms intermolecular hydrogen bonds and becomes hydrophilic at room temperature of around 30 °C. The hydrophilic patch with low contact angle allows the aqueous solution to flow through. This generates the “flow” condition of the valve. The “stop” and “flow” state of the valve can be achieved back and forth for multiple times via the cycle of heating–cooling–washing with DI water to remove the possible residue-drying.

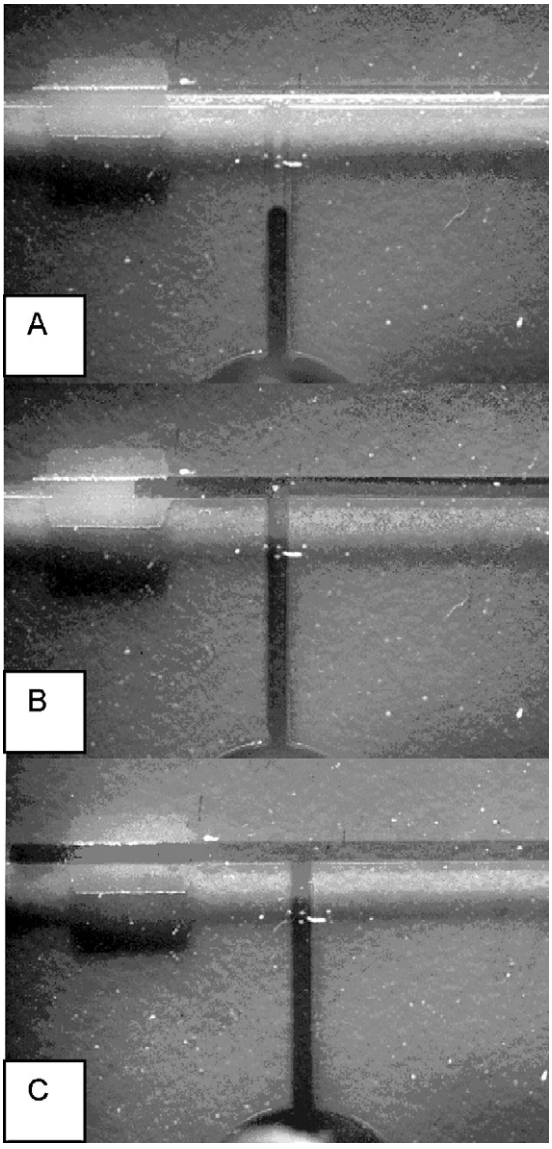

Fig. 7. The operation of superhydrophobic/hydrophilic valve (A) dyed water approaches to T-junction, (B) stops at the superhydrophobic patch at elevated temperature and (C) passes through the hydrophobic patch at room temperature.

4. Conclusions

In summary, conformal hydrophobic/hydrophilic and superhydrophobic/hydrophilic thermo-stimulated switchable surfaces were prepared and optimized for a wide range of wettability control by the layer-by-layer deposition of PAH and silica nanoparticles followed by surface modification. The surface characteristics including morphology and composition in relation to the wettability of the surface were studied. Using a novel synthesis and grafting route, a switchable polymer surface was fabricated and fully integrated into a microfluidic channel. A smart surface-based microvalve was created and tested through the combination of the layer-by-layer self-assembly technique and microfabrication, which promises various new applications in microflow regulation. Our future work will be based on integrating a micro-heater and channels for running cooling water into the device, which will help to decrease the time lag between the open and close status of the valve in the microfluidic channel.

Acknowledgments

This research has been partially supported by the National Science Foundation CAREER ECS 0348603 and CAREER DMR 0746499, and University of Central Florida (UCF) In-House Support.

References

[1] R.S. Martin, P.D. Root, D.M. Spence, Microfluidic technologies as platforms for performing quantitative cellular analyses in an in vitro environment, Analyst 131 (2006) 1197–1206.
[2] P.S. Dittrich, A. Manz, Lab-on-a-chip: microfluidics in drug discovery, Nat. Rev. Drug Discov. 5 (2006) 210–218.
[3] J. El-Ali, P.K. Sorger, K.F. Jensen, Cells on chips, Nature 442 (2006) 403–411.
[4] E.N. Gatimu, J.V. Sweedler, P.W. Bohn, Nanofluidics and mass-limited chemical analysis, Analyst 131 (2006) 705–709.
[5] H. Song, D.L. Chen, R.F. Ismagilov, Reactions in droplets in microfluidic channel, Angew. Chem. Int. Ed. 45 (2006) 7336–7356.
[6] H. Andersson, W. van der Wijngaart, P. Griss, F. Niklaus, G. Stemme, Micromachined flow-through filter-chamber for chemical reactions on beads, Sens. Actuators B: Chem. 75 (2001) 136–141.
[7] Y. Qing, J.M. Bauer, J.S. Moore, D.J. Beebe, Fabrication and characterization of a biomimetic hydrogel check valve, in: IEEE-EMBS Special Topic Conference on Microtechnologies in Medicine & Biology, 2000, pp. 336–339.
[8] D. Kim, D.J. Beebe, A bi-polymer micro one-way valve, Sens. Actuators A: Phys. 136 (2007) 426–433.
[9] H.G. Craighead, Nanoelectromechanical systems, Science 290 (2000) 1532–1535.
[10] H.O. Jacobs, A.R. Tao, A. Schwartz, D.H. Gracias, G.M. Whitesides, Fabrication of a cylindrical display by patterned assembly, Science 296 (2002) 323–325.
[11] V.V. Tsukruk, Assembly of supramolecular polymers in ultrathin films, Prog. Polym. Sci. 22 (1997) 247–311.
[12] D.M. Jones, J.R. Smith, W.S.T. Huck, C. Alexander, Variable adhesion of micropatterned thermoresponsive polymer brushes: AFM investigations of poly(*N*-isopropylacrylamide) brushes prepared by surface-initiated polymerizations, Adv. Mater. 14 (2002) 1130–1134.
[13] L.K. Ista, V.H. Perez-Luna, G.P. Lopez, Surface-grafted, environmentally sensitive polymers for biofilm release, Appl. Environ. Microbiol. 65 (1999) 1603–1609.
[14] N. Nath, A. Chilkoti, Creating "Smart" surfaces using stimuli responsive polymers, Adv. Mater. 14 (2002) 1243–1247.
[15] B.A. Buchholz, E.A.S. Doherty, M.N. Albarghouthi, F.M. Bogdan, J.M. Zahn, A.E. Barron, Microchannel DNA sequencing matrices with thermally controlled 'viscosity switch', Anal. Chem. 73 (2001) 157–164.
[16] T.P. Russell, Surface-responsive materials, Science 297 (2002) 964–967.
[17] G. de Crevoisier, P. Fabre, J. Corpart, L. Leibler, Switchable tackiness of liquid crystalline polymer, Science 285 (1999) 1246–1249.
[18] J.R. Matthews, D. Tuncel, R.M.J. Jacobs, C.D. Bain, H.L. Anderson, Surfaces designed for charge reversal, J. Am. Chem. Soc. 125 (2003) 6428–6433.
[19] K. Kim, W.S. Joen, J.K. Kang, J.W. Lee, S.Y. Jon, T. Kim, K. Kim, A pseudorotaxane on gold: formation of self-assembled monolayers, reversible dethreading and rethreading of the ring, and ion-gating behavior, Angew. Chem. Int. Ed. 42 (2003) 2293–2296.
[20] M.W.J. Prins, W.J.J. Welters, J.W. Weekamp, Fluid control in multichannel structures by electrocapillary pressure, Science 291 (2001) 277–280.
[21] N.L. Abbott, C.B. Gorman, G.M. Whitesides, Active control of wetting using applied electrical potentials and self-assembled monolayers, Langmuir 11 (1995) 16–18.
[22] M. Byloos, H. Al-Maznai, M. Morin, Phase transitions of alkanethiol self-assembled monolayers at an electrified gold surface, J. Phys. Chem. B 105 (2001) 5900–5905.
[23] T. Sun, G. Wang, L. Feng, B. Liu, Y. Ma, L. Jiang, D. Zhu, Reversible switching between superhydrophilicity and superhydrophobicity, Angew. Chem. Int. Ed. 43 (2004) 357–360.
[24] H.S. Lim, J.T. Han, D. Kwak, M. Jin, K. Cho, Photoreversibly switchable superhydrophobic surface with erasable and rewritable pattern, J. Am. Chem. Soc. 128 (2006) 14458–14459.
[25] S. Chia, J. Cao, J.F. Stoddart, J.I. Zink, Working supramolecular machines trapped in glass and mounted on a film surface, Angew. Chem. Int. Ed. 40 (2001) 2447–2451.
[26] V. Balzani, A. Credi, F.M. Raymo, J.F. Stoddart, Artificial molecular machines, Angew. Chem. Int. Ed. 39 (2000) 3348–3391.
[27] R. Ballardini, V. Balzani, A. Credi, M.T. Gandolfi, M. Venturi, Artificial molecular-level machines: which energy to make them work? Acc. Chem. Res. 34 (2001) 445–1445.
[28] K. Ichimura, S.K. Oh, M. Nakagawa, Light-driven motion of liquids on a photoresponsive surface, Science 288 (2000) 1624–1626.
[29] A.J. Pertsin, M. Grunze, H.J. Kreuzer, R.L.C. Wang, The effect of electrostatic fields on an oligo(ethylene glycol) terminated alkanethiol self-assembled monolayer, Phys. Chem. Chem. Phys. 2 (2000) 1729–1733.
[30] J. Lahann, S. Mitragotri, T.N. Tran, H. Kaido, J. Sundaram, I.S. Choi, S. Hoffer, G.A. Somorjai, R. Langer, A reversibly switching surface, Science 299 (2003) 371–374.
[31] G. Decher, Fuzzy nanoassemblies: toward layered polymeric multicomposites, Science 277 (1997) 1232–1237.
[32] S. Yang, M.F. Rubner, Micropatterning of polymer thin films with pH-sensitive and cross-linkable hydrogen-bonded polyelectrolyte multilayers, J. Am. Chem. Soc. 124 (2002) 2100–2101.
[33] S.A. Sukhishvili, S. Granick, Layered, erasable polymer multilayers formed by hydrogen-bonded sequential self-assembly, Macromolecules 35 (2002) 301–310.
[34] C. Yam, A.K. Kakkar, Molecular self-assembly of dihydroxy-terminated molecules via acid–base hydrolytic chemistry on silica surfaces: step-by-step multilayered thin film construction, Langmuir 15 (1999) 3807–3815.
[35] D. Li, Y. Jiang, C. Li, Z. Wu, X. Chen, Y. Li, Self-assembly of polyaniline/polyacrylic acid films via acid–base reaction induced deposition, Polymer 40 (1999) 7065–7070.
[36] L. Zhai, M.C. Berg, F.Ç. Cebeci, Y. Kim, J.M. Milwid, R.E. Cohen, M.F. Rubner, Patterned superhydrophobic surfaces: toward a synthetic mimic of the Namib Desert beetle, Nano Lett. 6 (2006) 1213–1217.
[37] F.Ç. Cebeci, Z. Wu, L. Zhai, R.E. Cohen, M.F. Rubner, Nanoporosity-driven superhydrophilicity: a means to create multifunctional antifogging coatings, Langmuir 22 (2006) 2856–2862.
[38] L. Zhai, F.Ç. Cebeci, R.E. Cohen, M.F. Rubner, Stable superhydrophobic coatings from polyelectrolyte multilayers, Nano Lett. 7 (2004) 1349–1353.
[39] R.M. Jisr, H.H. Rmaile, J.B. Schlenoff, Hydrophobic and ultrahydrophobic multilayer thin films from perfluorinated polyelectrolytes, Angew. Chem. Int. Ed. 44 (2005) 782–785.
[40] A.W. Neumann, R.J. Good, in: R.J. Good, R.R. Stromberg (Eds.), Experimental Methods in Surface and Colloid Science, vol. 11, Plenum, New York, 1979, pp. 31–91.
[41] L.E. Murr, In Interfacial Phenomena in Metals and Alloys, Addison Wesley Publ. Company, New York, 1974.
[42] R.N. Wenzel, Resistance of solid surface to wetting by water, Ind. Eng. Chem. 28 (1936) 988–994.
[43] R.N. Wenzel, Surface roughness and contact angle, J. Phys. Colloid Chem. 53 (1949) 1466–1467.
[44] A.B.D. Cassie, S. Baxter, Wettability of porous surfaces, Trans. Faraday Soc. 40 (1944) 546–551.
[45] H.G. Schild, Poly(*N*-isopropylacrylamide): experiment, theory and applications, Prog. Polym. Sci. 17 (1992) 163–249.
[46] G. Li, L. Shi, Y. An, W. Zhang, R. Ma, Double-responsive core-shell-corona micelles from self-assembly of diblock copolymer of poly(*t*-butyl acrylate-co-acrylic acid)-b-poly(*N*-isopropylacrylamide), Polymer 47 (2006) 4581–4587.
[47] D. Kuckling, H.J.P. Adler, K.F. Arndt, L. Ling, W.D. Habicher, Temperature and pH dependent solubility of novel poly(*N*-isopropylacrylamide) copolymers, Macromol. Chem. Phys. 201 (2000) 273–280.
[48] J. Huang, X.Y. Wu, Effect of pH, salt, surfactant and composition on phase transition of poly(NIPAm/MAA) nanoparticles, Polym. Sci. Part A: Polym. Chem. 37 (1999) 2667–2676.
[49] J. Bravo, L. Zhai, Z. Wu, R.E. Cohen, M.F. Rubner, Transparent superhydrophobic films based on silica nanoparticles, Langmuir 23 (2007) 7293–7298.
[50] L.K. Ista, S. Mendez, V.H. Perez-Luna, G.P. Lopez, Synthesis of poly(*N*-isopropylacrylamide) on initiator-modified self-assembled monolayers, Langmuir 17 (2001) 2552–2555.
[51] G. Londe, A. Chunder, A. Wesser, L. Zhai, H.J. Cho, Microfluidic valves based on superhydrophobic nanostructures and switchable thermosensitive surface for lab-on-chip (LOC) systems, Sens. Actuators B: Chem. 132 (2008) 431–438.